NASA TECHNICAL NOTE

NASA TN D-3402

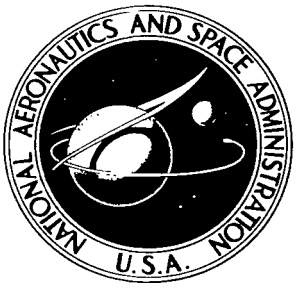

NASA TN D-3402

MANUAL ABORT GUIDANCE FROM THE MIDCOURSE REGION OF A LUNAR MISSION

by George P. Callas and Robert B. Merrick

Ames Research Center

Moffett Field, Calif.

NATIONAL AERONAUTICS AND SPACE ADMINISTRATION • WASHINGTON, D. C. • MAY 1966

MANUAL ABORT GUIDANCE FROM THE MIDCOURSE REGION OF A LUNAR MISSION

By George P. Callas and Robert B. Merrick

Ames Research Center
Moffett Field, Calif.

NATIONAL AERONAUTICS AND SPACE ADMINISTRATION

For sale by the Clearinghouse for Federal Scientific and Technical Information
Springfield, Virginia 22151 – Price $2.00

TABLE OF CONTENTS

	Page
SUMMARY	1
INTRODUCTION	1
SYMBOLS	2
DESCRIPTION OF THE PROBLEM	4
THE ABORT SYSTEM	5
Determination of the Vehicle's State	5
Determination of the Abort Trajectory	6
The Abort Implementation System	7
ERROR ANALYSIS	7
Estimation Errors	7
Abort Chart Computational Errors	8
Thrusting Errors	8
THE DIGITAL COMPUTER SIMULATION	10
Description of the System	10
The Trajectory Profile	11
The Simulated Emergencies	12
Error Assumptions	13
RESULTS AND DISCUSSION	13
Performance Criteria	13
Perigee Point Statistics	13
CONCLUSIONS	15
APPENDIX A - DERIVATION AND PRACTICAL IMPLICATIONS OF THE ABORT CHARTS	17
APPENDIX B - PRIMARY NAVIGATION SYSTEM	21
APPENDIX C - EQUATIONS OF MOTION	23
REFERENCES	25
TABLES	26
FIGURES	31

MANUAL ABORT GUIDANCE FROM THE MIDCOURSE REGION OF A LUNAR MISSION

By George P. Callas and Robert B. Merrick
Ames Research Center

SUMMARY

A manual abort system that incorporates charts for computing the vector abort velocity increment and a simplified Inertial Velocity Measurement Unit (IVMU) for monitoring the abort maneuver has been investigated and simulated on a digital computer. The charts derived from a four-body analysis of the abort problem are based on the concept of preselected abort points along a nominal lunar trajectory. The errors in implementing the abort maneuver are measured with the IVMU and a subsequent vernier velocity correction is made.

The prime objective of the abort system is to insure a return flight to a prescribed perigee point in the center of the earth's entry corridor. Of secondary importance is the system's capability of returning the vehicle to a desirable landing area. The ability of the system to achieve these objectives is demonstrated by simulating a lunar mission on the digital computer and assuming failures that necessitate abort at various points along the lunar trajectory. The abort performance is then evaluated according to the magnitude of end-point errors resulting from errors in the abort maneuver.

The principal errors considered are in knowing the vehicle's position and velocity before the abort maneuver and the thrusting errors during the abort and vernier maneuvers. The IVMU measurement errors are assumed to be negligible compared to the thrusting errors. The abort maneuvers are restricted to the original trajectory plane, and the velocity increments are assumed to be impulsive.

It is shown that aborts can result in safe returns for emergencies occurring in the region from lunar injection to well within the moon's sphere of influence, and that some degree of landing site control is possible if the emergency does not require a minimum return time.

INTRODUCTION

Manned space flights must have a very high probability of mission success, and an even higher probability of crew survival. The emphasis on crew survival points up the need for abort techniques and subsystems that will enable a safe return from all phases of the mission in any event other than a catastrophe.

In general, any failure necessitating an abort will impose constraints on the abort maneuver. For example, a power failure could disable both the

communications link and the on-board computer, making manual abort computations necessary. The severity of the failure will dictate whether an immediate return is essential or some secondary mission is possible. A general problem is to determine the simplest abort system that will enable a safe return from the midcourse region when an immediate return is desired.

The principal objective of this study is to investigate a specific system that evolved from previous abort studies. In the abort study of reference 1, a method was developed for calculating the abort guidance for minimum return time. The family of solutions generated by assuming various abort velocity capabilities was presented as hodographs, and it was noted that these hodographs could be used for graphic solutions of the abort trajectory. The utilization of this technique in a manual abort system was reported and some results were presented in reference 2. The possibility of using precomputed charts to control the landing site was also described. However, the end-point uncertainties associated with errors in executing the abort were not analyzed. The abort system of reference 2 requires, as inputs, the vehicle's range and velocity, and the performance figures quoted reflect, to some degree, the performance of the assumed primary system which supplies these quantities. The observation schedule used for this system was not optimized for the abort system; therefore, the abort performance was in some cases marginal or unacceptable.

In the present study the work of reference 2 is amplified with specific considerations given to the following areas: (1) A primary system employing sextant observations rather than theodolite observations, (2) the primary system observation schedule which is favorable for the abort requirements, (3) manual aborts incorporating landing site control, and (4) the end-point errors in altitude, downrange, and crossrange.

SYMBOLS

E covariance matrix of errors due to delay in applying the vernier correction

I identity matrix

k observation number

K weighting matrix

M transformation matrix

n abort number

P covariance matrix of estimation error vector

R range from earth

R_p reference perigee

δR	position deviation
δR_p	perigee deviation
S	covariance matrix of abort velocity correction error
t	time
T	covariance matrix of vernier velocity correction error
$\underline{u}$	unit vector
V	velocity
δV	velocity deviation
ΔV	magnitude of abort velocity increment
$\Delta\hat{\underline{V}}$	commanded abort velocity increment
$\hat{\underline{x}}$	estimated state of the vehicle (six vector)
γ	velocity correction pointing error, rms
ϵ	velocity correction cutoff error, rms
Θ	angle of abort velocity vector from radial direction
κ	velocity correction proportional error, rms
μ_e	gravitational parameter for the earth
σ	standard deviation of sextant error
Φ	state transition matrix

Notation Conventions

$( )^T$	transpose of matrix ( )
$\bar{( )}$	expected value of ( )
$\underline{( )}$	vector of ( )

Subscripts

a	abort point
e	end point of abort reference trajectory

H	horizontal
k	based on first k observations
m	abort trajectory number
max	maximum
min	minimum
n	based on the nth abort point
N	normal
o	initial value
p	perigee
R	radial
t	time
v	vernier correction point

DESCRIPTION OF THE PROBLEM

The abort is a navigation problem, the aspects of which are described as follows. Consider a manned spacecraft on a typical lunar mission as illustrated in sketch (a). Suppose that at some point along the trajectory (e.g., point A) a failure occurs necessitating an abort. First, it is necessary to

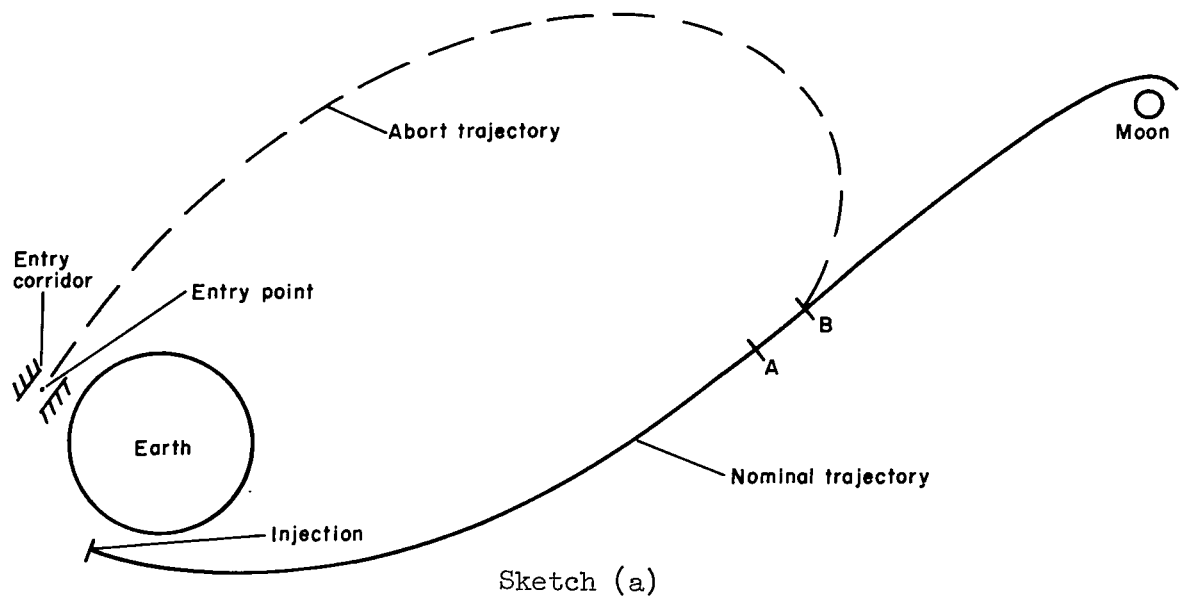

Sketch (a)

determine the vehicle's state (position and velocity) at an abort point (e.g., point B) occurring at a time after point A. Second, an abort trajectory must be selected and the required abort maneuver computed. Third, the correct maneuver must be executed and the desired trajectory achieved so that the vehicle will return to the center of the entry corridor.

Any failure that necessitates an abort will impose constraints on the abort maneuver; therefore, certain ground rules for the abort system have been postulated as follows:

1. The principal objective of the abort is a safe return to earth (return to a specified geographical area is desirable but secondary). Thus, accuracy in achieving a safe entry, or more specifically in achieving the prescribed entry corridor, is required even in the event of a primary guidance system failure.

2. To provide increased safety for the crew, the abort shall be accomplished without ground communications, and shall not require the use of the primary navigation system after the emergency.

3. All manual computations that are required must be simple yet accurate and demand little time, allowing the crew to devote their attention to other problems resulting from the emergency.

4. The number of points along the trajectory at which aborts may be initiated is limited and their locations fixed prior to the flight. These locations will be called abort points.

5. The abort maneuvers are restricted to in-plane maneuvers and the velocity increments are assumed to be impulsive.

The abort system that was used in this study and that satisfies the constraints imposed by the above ground rules is described below.

THE ABORT SYSTEM

The abort system is considered as three subsystems, each of which solve a portion of the abort problem discussed earlier. The three subsystems are: (1) a state determination system, (2) an abort trajectory determination system, and (3) an abort implementation system.

Determination of the Vehicle's State

Before the abort maneuver can be computed, the abort initial conditions must be available. The specific quantities necessary for the abort system under investigation are the vehicle's radial and horizontal components of velocity, and the time the vehicle reaches the abort point. The abort points are selected prior to the flight, and the primary navigation system can be used to predict periodically the abort initial conditions at these points. In this study the primary navigation system is programmed to predict these

quantities for the two successive abort points each time a new observation is processed. The second point is used when the failure occurs too near the first abort point. Thus, a current estimate of the abort initial conditions is available even in the event of a primary system failure.

Determination of the Abort Trajectory

The abort trajectory determination system consists of a catalog of abort charts. Basically, the abort charts contain the initial conditions of all the planar abort trajectories of interest that originate at the reference abort point and result in safe return trajectories. The following table is for a typical abort point and illustrates the basic information required on the abort charts.

Abort range, 205,000 km

Abort trajectory, m	Radial velocity, V_{Rm}	Horizontal velocity, V_{Hm}
1	0.60136381	0.34781977
2	-.23285700	.34787860
3	-1.43762580	.34792792

The first column is simply an identification number for the various trajectories that are cataloged. Three trajectories are illustrated in the table. The second and third columns list the velocity that is required at the specific abort point which, in this example, is at a range of 205,000 km. The particular abort trajectory chosen will depend on the constraints imposed by the emergency requiring the abort. One trajectory might represent the minimum return time solution while others may offer minimum fuel expenditures or solutions that return to specific areas. A discussion of the derivation and the practical implications of the abort charts is presented in appendix A. Once the abort trajectory is selected, the abort maneuver is computed by simply differencing each component of velocity given in the abort chart with the corresponding value predicted by the state determination system previously described. Symbolically, if the subscript o denotes the vehicle's predicted state at the abort point, and the subscript m denotes the abort trajectory number ($m = 1, 2, 3$ for the example shown in the above table), then the abort velocity increment in the radial and horizontal directions (ΔV_R and ΔV_H, respectively) is given by

$$\left.\begin{aligned} \Delta V_R &= V_{Rm} - V_{Ro} \\ \Delta V_H &= V_{Hm} - V_{Ho} \end{aligned}\right\} \tag{1}$$

and the direction of thrust application, θ, measured from the radial direction and in the orbit plane is given by

$$\theta = \tan^{-1} \frac{\Delta V_H}{\Delta V_R} \tag{2}$$

The Abort Implementation System

After the abort trajectory is determined and the abort maneuver is computed, the vehicle must be oriented in the proper direction and the desired maneuver implemented. Since the primary system may be inoperable after the emergency, the vehicle orientation and the abort implementation must be accomplished with a backup system. One possible system consists of an optical device directly coupled to an Inertial Velocity Measurement Unit (IVMU). This can be a simple system since one of the velocity components to be measured is radial; consequently, manual alinement is possible. To aline the vehicle and measure the abort velocity increment, it is necessary to establish the orbital plane. During the primary mode of operation the orbit plane is known; therefore reference stars in the orbit plane may be recorded for use in the event of an abort. If the emergency occurs before the primary mode of operation is activated, one technique for establishing the orbital plane would be to observe the earth's track in the star background. For an abort that occurs early in the flight, the motion of the earth in the star background is rapid and this technique should be relatively accurate.

Errors in thrusting during the abort maneuver can cause large deviations from the desired return trajectory and must be corrected by subsequent maneuvers (cf. ref. 1). Since the IVMU can measure the implemented velocity more accurately than it can be applied, the errors in making the abort maneuver may be measured and corrected subsequently with a vernier engine that can be controlled accurately.

ERROR ANALYSIS

Before a meaningful evaluation of the abort system can be made, the errors inherent in the abort system must be analyzed and an appropriate error model derived. The errors introduced by each of the abort subsystems are described below, and the error model used for computing the resulting end-point errors is developed.

Estimation Errors

The errors in estimating the vehicle's state before the abort depend upon the primary navigation system. The system assumed for this study is described in appendix B. Basically, sextant measurements between known stars and the earth and moon are inputs, and the vehicle's estimated state, $[x]$, with a covariance matrix of errors in estimation, $[P]$, are primary outputs. An integral part of the system is an integration subroutine which is used to project the vehicle's current estimated state to the following two preselected abort ranges. At each of these abort points three quantities are displayed, the radial velocity, the horizontal velocity, and the time the vehicle will achieve the abort range. The velocity components are used as initial conditions for computing the abort maneuver which, when executed, will place the vehicle on a new trajectory.

To obtain the end-point errors resulting from the errors in estimating the abort initial conditions, the error matrix (P-matrix) is updated from the

last observation to the abort point. This updated error matrix is taken as the injection error matrix for the abort trajectory which starts at the reference abort range. Hence, if P_k represents the covariance matrix of estimation errors after the kth observation has been processed, the updated error matrix at the nth abort point, P_n, is obtained from

$$P_n = \Phi(t_n,t_k)P_k\Phi^T(t_n,t_k) \tag{3}$$

where $\Phi(t_n,t_k)$ is the state transition matrix from the observation time, t_k, to the abort time, t_n. The covariance matrix P_n of injection errors for the abort leg of the trajectory is transferred to the end point by the transition matrix of the abort reference trajectory

$$P_e = \Phi(t_e,t_n)P_n\Phi^T(t_e,t_n) \tag{4}$$

Equation (4) represents the end-point statistics at perigee of the abort trajectory in the inertial coordinate system. These statistics are transformed to obtain the position and velocity variance in terms of perigee altitude, downrange, and crossrange. Thus,

$$P_{R_p} = MP_eM^T \tag{5}$$

where M is the transformation matrix relating the inertial system to the perigee reference system. The trace of equation (5) yields the three position and three velocity variances.

Abort Chart Computational Errors

The abort trajectory is computed from charts that are compiled prior to flight. It is possible to achieve sufficient accuracy in the model of the physical system to virtually eliminate the computational errors. Thus the error contribution from this source is negligible and is not included in the error model.

Thrusting Errors

The implementation of the abort maneuver introduces additional errors that will affect the miss at the end point. The statistical error model used in this study is derived in appendix A of reference 3. The thrusting errors considered are those in pointing and in thrust magnitude. When the computed abort maneuver is implemented it is recognized that a large error in thrust magnitude may occur if manual shutoff is necessary. Since the implemented maneuver can be measured much more accurately than it can be applied, a vernier correction is made after the abort maneuver. This correction is made with a smaller engine that can be controlled more accurately so the resultant thrusting error is the vector sum of the measurement errors and vernier thrusting errors as

shown in sketch (b). The measurement errors are small and analogous to vernier thrusting errors; therefore in this analysis they are considered part of the vernier thrusting errors.

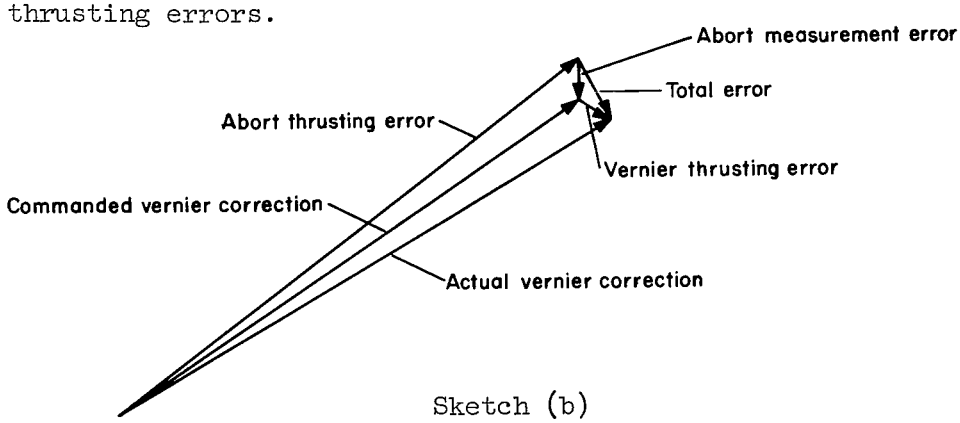

Sketch (b)

The covariance matrix of vector uncertainty, S, in making the commanded abort maneuver, $\Delta\hat{\underline{V}}$, is given by equation (A17) in reference 3. This equation may be written as

$$S = \frac{\overline{\gamma^2}}{2}\left(\overline{\Delta\hat{V}^2}I - \overline{\Delta\hat{\underline{V}}\,\Delta\hat{\underline{V}}^T}\right) + \left(\overline{\kappa^2} + \frac{\overline{\epsilon^2}}{\overline{\Delta\hat{V}^2}}\right)\overline{\Delta\hat{\underline{V}}\,\Delta\hat{\underline{V}}^T} \tag{6}$$

where $\overline{\gamma}$ is the expected value of the aiming error, $\overline{\kappa}$ is the expected value of an error along the thrust vector proportional to its magnitude, and $\overline{\epsilon}$ is the expected value of the cutoff error also assumed to be along the thrust vector. If the vernier correction is applied immediately after the abort maneuver, equation (6) represents the statistics of the desired vernier correction, and the trace of S represents the variance of the vernier velocity magnitude. Thus, the thrusting error, T_{t_a}, after an abort maneuver with a simultaneous vernier correction, applied at time, t_a, is given by

$$T_{t_a} = \frac{\overline{\gamma^2}}{2}\left[TR(S)I - S\right] + \left[\overline{\kappa^2} + \frac{\overline{\epsilon^2}}{TR(S)}\right]S \tag{7}$$

where TR(S) represents the trace of S, and I is the identity matrix. However, the vernier correction is actually applied at a later time so an error is introduced since the correct vernier correction at the later time is slightly different. If $\Phi(t_v,t_a)$ is the state transition matrix along the abort trajectory from the abort time, t_a, to the time of the vernier correction, t_v, then the covariance matrix of the error that is introduced, E, is given by

$$E = \left[\Phi(t_v,t_a) - I\right]S\left[\Phi(t_v,t_a) - I\right]^T \tag{8}$$

The covariance matrix of the total thrusting error at time t_v is the sum of equations (7) and (8)

$$T_{t_v} = \frac{\overline{\gamma^2}}{2}\left[TR(S)I - S\right] + \left[\overline{\kappa^2} + \frac{\overline{\epsilon^2}}{TR(S)}\right]S + E \tag{9}$$

The thrusting error statistics of equation (9) are projected to the end point of the abort trajectory by

$$T_e = \Phi(t_e,t_v)T_{t_v}\Phi^T(t_e,t_v) \tag{10}$$

and equation (10) is transformed into the perigee coordinate system, as in equation (5), to obtain the desired statistics. Thus,

$$T_{R_p} = MT_eM^T \tag{11}$$

THE DIGITAL COMPUTER SIMULATION

To evaluate the performance of the abort system, a lunar mission was simulated on the digital computer, and primary system failures requiring abort were assumed at various points along the trajectory. After each failure the vehicle was allowed to continue to an abort point, at which time an abort was executed placing the vehicle on an earth-bound trajectory. The errors in estimating and abort thrusting were computed and projected to the return reference perigee where they were examined in a statistical sense.

Description of the System

A block diagram of the simulation is shown in sketch (c). The system is separated into three parts by dashed lines. The top block labeled "Physical system" represents the vehicle's actual trajectory, celestial observations, and

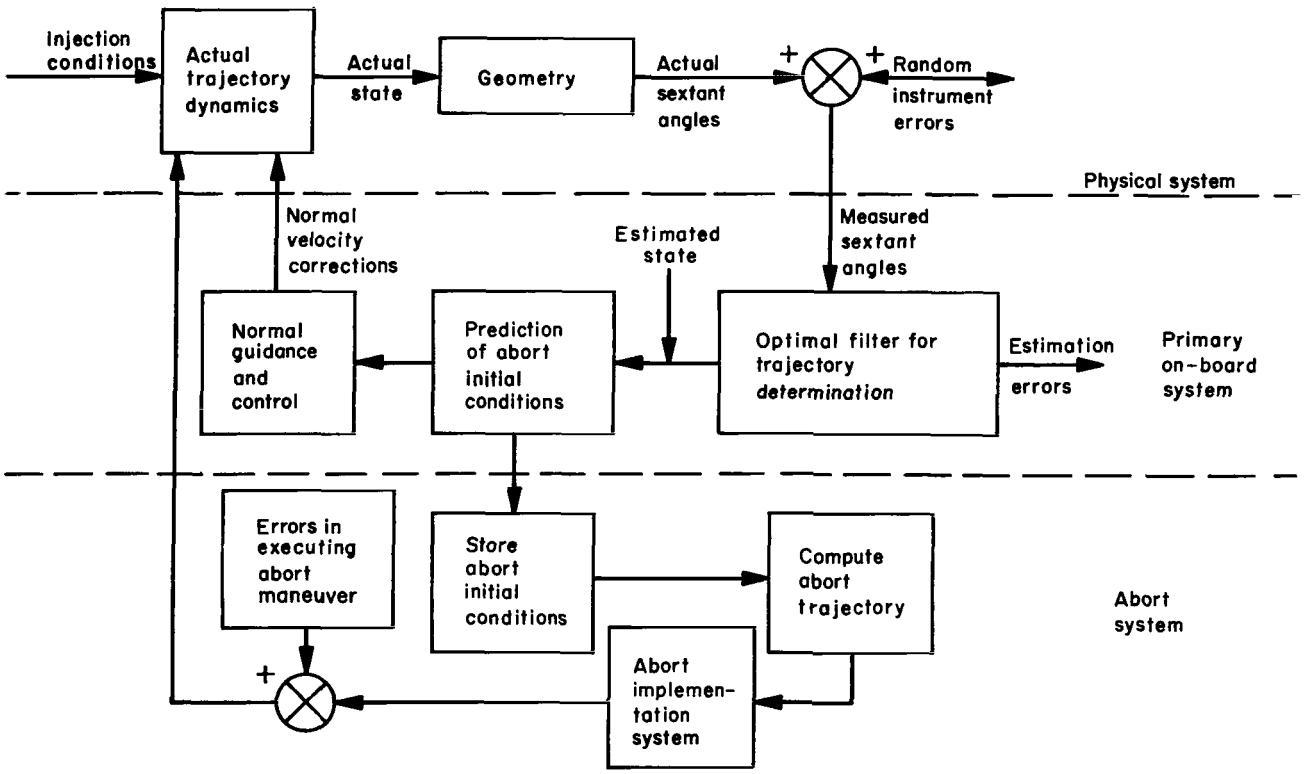

Sketch (c)

instrument errors which generate the measured sextant angles. For this study the actual trajectory is the solution of the four-body nonlinear equations of motion in the geocentric nonrotating Cartesian coordinate system. The equations of motion, together with a brief description of the coordinate system and the trajectory computation, are given in appendix C.

The measured sextant angles are simulated by taking the actual angles determined from the actual trajectory and corrupting them with additive noise. These angles are then used as inputs to the primary on-board system which is represented by the middle block of sketch (c). In the normal mode of operation, the primary system is idle until an observation is made, at which time the system processes this new observation to obtain a new estimate of the vehicle's state. The new estimated state is projected ahead to the next two preselected abort ranges and new abort initial conditions are stored for these two points. This process is repeated with each new observation so that current abort conditions are always available for an abort.

The lower portion labeled "Abort system" contains the logic for determining the abort velocity from the precomputed data and the stored abort initial conditions. When an abort maneuver is necessary, the abort logic selects the stored abort initial conditions and the appropriate precomputed data, computes the required abort maneuver, and initiates the abort mode. The vehicle is allowed to continue on its original trajectory until the predicted abort range is achieved. At this point, the abort maneuver is implemented, placing the vehicle on an earth-bound trajectory. The blocks labeled "Abort implementation system" and "Errors in executing abort maneuver" represent the mechanization of equation (9). After the abort and vernier corrections have been applied, the estimation and thrusting error statistics are projected to the end point for examination.

The Trajectory Profile

All the reference trajectories discussed in this study originate from the reference lunar trajectory shown in figure 1. This trajectory is entirely ballistic and is inclined approximately 20° from the moon's orbital plane. Injection occurs at perigee on February 11, 1966 with an altitude of 120 km at about 99.46 percent of escape velocity. If no abort is executed the vehicle will pass ahead of the moon and achieve a perilune at a lunar altitude of 185.2 km (100 nautical miles) 70.68 hours after injection. The observation and velocity correction schedule for the outbound leg of the trajectory is listed in table I.

The numbered points on the reference lunar trajectory of figure 1 represent the origin of the precomputed abort trajectories, and the dashed lines from three of the abort points illustrate typical abort trajectories. The precomputed abort points are spaced approximately 4 hours apart; the first point is about 2 hours from injection, and the last, about 58 hours. The selection of the abort points used in this study was somewhat arbitrary since the purpose of the study was to demonstrate a manual abort technique rather than optimize the location or number of abort points.

The determination of the end-point statistics requires the use of a reference abort trajectory as well as a reference lunar trajectory. A reference abort trajectory that returns to one of three landing sites was determined for each of the abort points. These solutions were found in the process of determining the abort charts and do not necessarily represent desirable landing sites. However, the use of these sites as target points demonstrates the feasibility of landing site control. A description of the abort trajectories, listing the location of all the abort points considered in this study, the abort velocity necessary to achieve the reference abort trajectory, and the landing site of each of the abort trajectories, is given in table II.

The Simulated Emergencies

Abort performance is evaluated for emergencies requiring abort at various points along the reference trajectory, and the end-point miss resulting from the abort is examined. The emergencies are assumed to occur at "critical" points known to give less satisfactory results, that is, at points where the covariance matrix of errors in estimating the state vector is greatest. This generally occurs before a sequence of observations. Figure 2 illustrates an enlarged portion of the trajectory with the observation schedule and abort points. The points numbered 1-4 represent the first four abort points and the stars represent emergencies at the "critical" points. Any emergency occurring after injection and before the first observation would result in an abort at the first abort point, and the uncertainty in estimating the injection errors would be the major source of error in perigee miss. If the emergency were to occur after an observation had been processed, the end-point error would be smaller since each observation reduces the error in the estimated state.

If an emergency were to develop very near an abort point, there would not be sufficient time to perform calculations and maneuver the vehicle for an abort. The abort would, therefore, have to be made at the next abort point. However, none of the scheduled observations could be made after the emergency, so the error existing after the last observation has to be projected to the next abort point to determine the uncertainty in estimation at that point. In this study it was assumed that 15 minutes is required to prepare for an abort maneuver; thus, if the emergency occurs within 15 minutes of an abort point, the abort is delayed until the following point.

Another type of "critical" point would occur if an emergency arose immediately after a velocity correction because additional uncertainties are introduced by the velocity correction. Table III defines the emergency points considered and the abort range where the abort was initiated for that emergency.

Error Assumptions

The nominal values of the assumed errors pertinent to this study are:

Injection errors (rms values):
1 km and 1 m/sec in each of the three directions in geocentric coordinate system

Abort thrusting errors (rms values):
1 percent in magnitude of correction
0.5° in direction
0.2 m/sec in cutoff

Vernier thrusting errors (rms values):
0.5 percent in magnitude
0.5° in direction
0.2 m/sec in cutoff

Sextant error (rms values):
$\sigma = \sqrt{100 + (0.001\alpha)^2}$ sec of arc
α = one-half the subtended angle of earth or moon

RESULTS AND DISCUSSION

Performance Criteria

Some criteria must be adopted for evaluating abort system performance. Since the prime objective after an abort is to return to earth within the entry corridor, the deviations from the center of the corridor are considered a measure of the performance of the system. It is convenient to express the center of the corridor in terms of the vacuum perigee, and the deviations from the center of the corridor as deviations in perigee altitude. A corridor of ±35.4 km (±22 statute miles) with center at a radius of 6430.0 km was assumed for this study. This corridor, obtained from reference 4, is for an entry vehicle with an L/D ratio of ±0.47 with a 10g maximum acceleration limit. If a 3σ deviation of ±35.4 km is assumed, the allowable 1σ perigee miss becomes 11.8 km (7.33 statute miles). Thus, a satisfactory entry is assumed to result if the perigee of the return trajectory is 6430.0 ± 11.8 km.

Perigee Point Statistics

The perigee errors that result from the emergencies at the critical regions defined in table III are listed in table IV. Columns 1 and 2 of table IV give the emergency conditions and abort points; columns 3-8 list the rms perigee miss resulting from the various error sources considered; and column 9 lists the rms time deviation between actual and reference perigee. Columns 6-8 give the total rms error in perigee altitude, downrange, and cross-range, respectively. The most pertinent error is the perigee altitude miss since this is a measure of the abort system performance. The three components whose rms sum make up the perigee altitude miss are listed in columns 3-5.

The rms perigee altitude miss due to the error in the knowledge of the state vector before the abort is tabulated in column 3. As expected, the results are poorest shortly after injection and before sufficient time has elapsed to complete the first sequence of scheduled observations. However, even the worst case, emergency condition 2, is sufficiently small so that the total perigee altitude error remains below the allowable error of 11.8 km. It should be emphasized that the observation schedule of the primary navigation system used in this study was chosen to enhance the performance of the abort system, and that an arbitrary observation schedule, that is, the schedule of reference 2, would not generally yield satisfactory results for all the aborts considered. The primary navigation system performance was evaluated with the observation schedule of this study, and it was determined that the performance was not significantly affected by the altered observation schedule.

The rms perigee altitude miss, due to the vernier thrusting error, tabulated in column 4, increases with increasing abort range. This too is as expected since the trajectory sensitivity coefficients increase as the time to go increases. The vernier thrusting error is the major contributor to the total perigee altitude error for the later aborts, and, therefore, this error will dictate the range beyond which manual aborts are not feasible without subsequent midcourse navigation and guidance.

The rms perigee altitude miss, due to a delay in making the vernier correction, is tabulated in column 5. This error is a function of the position on the trajectory as well as the delay between the abort maneuver and the vernier correction. For a delay time of 9 minutes, which was assumed in this study, the delay error contribution is significant but not critical to any of the abort conditions.

The total altitude miss given in column 6 is the root sum square of the three components listed in columns 3, 4, and 5. As mentioned earlier, the total altitude miss is the most pertinent, since the safety of the entry depends upon the magnitude of this error. The maximum value encountered was 10.73 km which is below the allowable error of 11.8 km.

The total rms perigee downrange error is tabulated in column 7. It should be emphasized that this downrange error is, by definition (eq. (5)), the rms horizontal deviation from reference perigee at the time of reference perigee. This error is significant in determining the rms time deviation between actual and reference perigee, which will be discussed later; however, it gives a poor indication of the deviation of the actual perigee from the reference perigee. If the deviation of the actual perigee from the reference perigee is assumed to be an independent linear function of the deviations in the state vector at the time of reference perigee, a simple relationship giving the altitude, downrange, and crossrange deviations of the actual perigee can be derived. This relationship, given in reference 5 (eq. (35)), is in the notation of the present report,

$$\delta\underline{R}_p = \left(\underline{u}_R\underline{u}_R^T + \underline{u}_N\underline{u}_N^T\right)(\delta\underline{R}) - \frac{R_p}{V_p}\left(\underline{u}_H\underline{u}_R^T\right)(\delta\underline{V})$$

It was evaluated and the rms altitude and crossrange deviations of actual perigee were found to be identical to the deviations at reference perigee time. However, the downrange deviation represents the rms horizontal separation of the actual and reference perigee points. These downrange deviations are negligibly small, indicating that the actual and reference perigees occur at nearly the same point. In all cases these deviations were 1.2 km or less.

The total rms perigee crossrange error is tabulated in column 8. The crossrange error generally decreases with increasing abort range, although all of the crossrange errors are negligible compared to the other total errors listed. The tendency for range errors to decrease with increasing range can be likened to a lever arm and fulcrum device. The earth's center is the fulcrum and the short arm is the constant perigee distance. As the lever arm increases in length (increasing range), constant deviations of the lever arm produce successively smaller motions of the object arm. This results in a decrease in range errors proportional to R_p/R. The crossrange errors are small because (1) in-plane velocity correction errors do not affect the crossrange error and (2) the out-of-plane velocity correction error is small compared to the magnitude of the total velocity vector so that only a small rotation of the trajectory plane is possible.

As mentioned previously, the downrange errors listed in column 7 give a poor indication of the deviation of the actual perigee. However, the time deviation between actual and reference perigees is very nearly the quotient of the downrange error of column 7 and the reference perigee velocity. This rms error is tabulated in column 9. Since the actual and reference perigees occur at approximately the same point in inertial space, the amount the earth rotates in this time deviation represents the significant landing site error. The earth's rotational rate is approximately 24 km/min so that these errors vary between 22 and 91 km. Such errors are well within the landing footprint of proposed lunar vehicles (ref. 6).

It is interesting to note that the downrange errors of column 7, and consequently the timing errors in column 9, tend to decrease with increasing abort range. No simple explanation has been found for this trend.

CONCLUSIONS

A manual abort system has been described and evaluated by simulation on a digital computer. From the results of this study the following conclusions can be given.

1. A tabulated representation of abort solutions for manual computation of abort initial conditions is both feasible and practical.

2. The manual task of computing the abort trajectory requires only simple arithmetic computations and the evaluation of a trigonometric function.

3. An analysis of errors including trajectory initial condition errors, primary navigation system errors, abort thrusting errors, and vernier thrusting errors indicates that the 3σ rms error in achieving the center of the entry corridor is less than 35.4 km.

4. The error in estimating the abort initial conditions depends on the observation schedule of the primary navigation system; therefore, the location of the abort points should be considered when this schedule is determined.

5. Since the abort and vernier velocity corrections can be measured more accurately than they can be made, the performance of the abort system is limited by vernier thrusting errors. A substantial improvement in the abort system performance would be realized, for ranges of 200,000 km or more, if these vernier thrusting errors were reduced.

6. The downrange and crossrange errors resulting from aborts chosen to return to specific landing sites is well within the landing footprint of entry vehicles with L/D ratios of 0.4-0.5.

Ames Research Center
National Aeronautics and Space Administration
Moffett Field, Calif., Feb. 11, 1966

APPENDIX A

DERIVATION AND PRACTICAL IMPLICATIONS OF THE ABORT CHARTS

The abort charts are based on the gravitational effects of the earth (including the second and fourth harmonic terms of the earth's oblateness) on the vehicle and on a spherical and homogeneous moon and sun. The technique used in determining the four-body abort charts employs a four-body digital program incorporating a two-body solution to initiate an iteration which converges to the desired four-body velocities. Similar techniques have been used for some time now for determining n-body space trajectories. This calculation is carried out for each abort solution and at each abort range. Thus, the abort charts contain discrete information which is tabulated to obtain the necessary degree of accuracy. However, for this discussion it is convenient to consider all possible solutions that meet the problem constraints, and the locus of all such solutions, at a given range, represents a special hodograph in the velocity plane. It is convenient to discuss the implications of the various solutions in terms of the two-body hodograph for which an analytic expression exists. The discussion is generally valid for the four-body hodograph, but where there are differences they are emphasized.

The analytic expression for the two-body hodograph is given by equation (1) of reference 1 and can be written as

$$V_H^2 = \frac{R_p^2}{R^2 - R_p^2} V_R^2 + \frac{2\mu R_p}{R}\left(\frac{1}{R + R_p}\right) \qquad (A1)$$

Since the gravitational parameter, μ, is a constant, and the center of the entry corridor specifies the desired radius of perigee, R_p, the velocity components, V_R and V_H, that satisfy equation (A1) can be determined for any value of range, R. The hodographs traced by equation (A1) are hyperbolas symmetrical about the V_R and V_H axes. In reference 1 it was shown that the left-hand branch of the hyperbolas represents "retrograde trajectories" which are undesirable and will not be considered as possible solutions in this discussion. A typical hodograph with the left-hand branch omitted is shown in sketch (d). Also shown in sketch (d) is the range of eccentricities, e, which indicates whether the solution yields an elliptic, parabolic, or hyperbolic trajectory. The solution on the V_H axis represents the minimum eccentricity solution and even

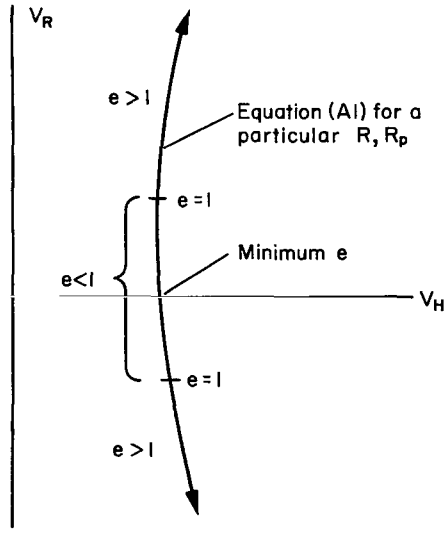

Sketch (d)

for relatively large abort velocity capabilities, minimum e remains greater than 0.8. The solutions above the V_H axis and below the e = 1 point represent "apogee passage" trajectories, while all those below the V_H axis are "direct return" solutions. Sketch (e) depicts the hodograph of sketch (d) with the addition of the vehicle's velocity vector before abort, V_o, and the abort velocity increment capability represented by the circle. Graphically, the achievable velocities which will provide a safe entry are those that lie within the circle and also on the hodograph plot of sketch (e). The dashed abort velocity vector labeled, ΔV, represents the minimum time solution. The dotted vector drawn from the head of the V_o vector perpendicular to the hodograph curve represents the minimum fuel solution (minimum ΔV). The return flight time associated with the minimum ΔV solution can be several days longer than that associated with the minimum return time solution. However, even with this large variation of flight time the inertial location of perigee remains nearly constant. This fact enhances the use of abort velocity magnitude as a means of landing site control. To illustrate this point, suppose the landing point for a particular solution is represented by point 1 in figure 3 after the vehicle has traversed a range angle of 35° from the entry point. If the abort velocity increment were reduced slightly so that the return flight time were increased by 1 hour, the vehicle's entry track would be similar to the first but shifted 15° (the earth's rotational rate) so that the vehicle would land at point 2 of figure 3. The solutions for points 1 and 2 are also represented on the hodograph of sketch (e). Every point between 1 and 2 on the hodograph of sketch (e) has a corresponding landing point in figure 3. Furthermore, if the return flight time is increased by up to 24 hours, the longitude of the landing point can be varied a full 360°.

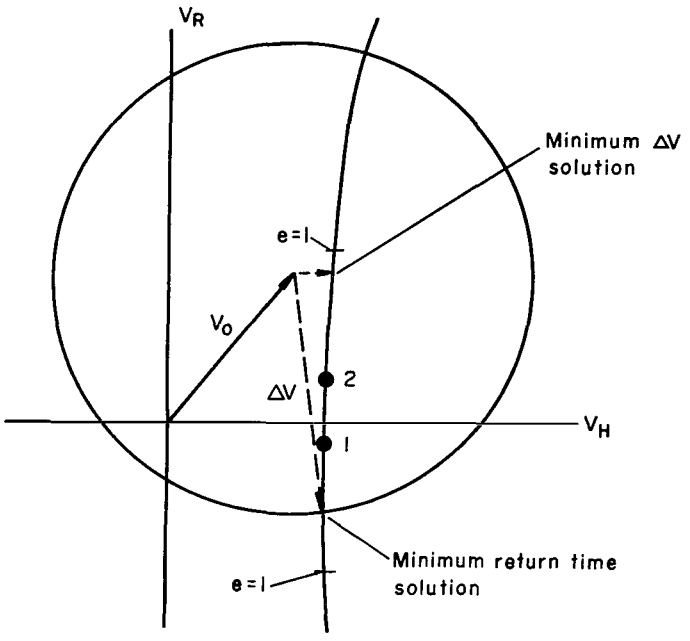

Sketch (e)

Since only planar aborts are considered, control of the landing latitude is much more limited, and this limited control is obtained by maneuvering during entry to change the entry range. The entry range capability of the entry vehicles should certainly be considered in compiling the abort charts since maneuvering during the entry phase is possible for a large class of midcourse aborts.

It should be emphasized that the aborts are initiated at specific ranges rather than specific times. This makes the two-body hodographs completely independent of the nominal trajectory since all the solutions result in a safe vacuum perigee (entry corridor). However, the landing site solutions are determined from a nominal trajectory which has associated with each abort

range a corresponding time. Deviations in this time result, to a first approximation, in errors proportional to the earth's rotational rate (15°/hr). This rate results in a maximum landing site error of 1600 km/hr of time deviation. Time errors of this magnitude can result from a launch delay or from an extremely bad translunar injection with no subsequent midcourse correction. If it is desirable to maintain landing site control for errors of this magnitude, nominal trajectories must be determined at time intervals sufficiently close to reduce the landing site error to an acceptable level. The hodograph for the two-body problem (except for the location of the landing site points) remains constant for all nominal trajectories. On the other hand, in the four-body problem the hodograph for each nominal trajectory varies as does the location of the landing site points. Thus, deviations from the nominal trajectory produce errors in perigee altitude in addition to the error in landing site. However, even the four-body hodographs have some element of generality that renders them valid for reasonable deviations from the nominal trajectory. Consider the hodographs shown in sketch (f). The solid curve represents a

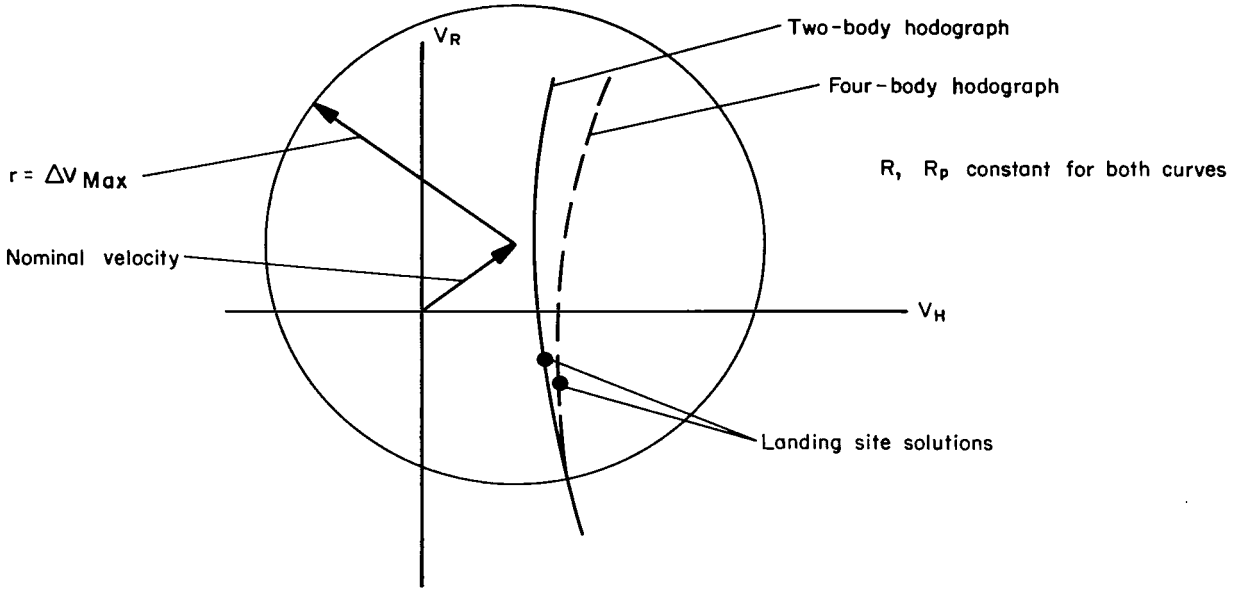

Sketch (f)

two-body hodograph and the dashed curve represents an exaggerated equivalent four-body hodograph. The labeled point shown on each of the curves represents the same landing site solution for the two- and four-body theory. The predominant perturbation is attributed to the moon, and for lunar missions, such as Apollo; this perturbation always tends to "deflect" the hodograph to the right as shown in sketch (f). Since the earth-moon-sun-vehicle geometry does not change significantly, even when trajectories vary by several hours from the nominal, the four-body hodographs remain valid for determining safe abort trajectories. However, as in the two-body theory, the landing site solutions are not valid for deviations from the nominal.

The difference between the two hodographs depends on the range at which the abort is made and the radial velocity of the vehicle after the abort maneuver. If the abort is made near the earth and the radial velocity after

the abort is small or negative (decreasing range), then the perturbations become negligible and the problem is essentially a two-body problem. If the abort occurs near the moon, the separation between the two- and four-body hodograph depends on the radial velocity after the abort. Obviously, if the vehicle's radial velocity is large and directed toward the earth, the return flight time would be small and the influence of the perturbing bodies would be very small.

Perturbations caused by the sun and the earth's oblateness are small compared to those caused by the moon. However, for some aborts these cannot be neglected. The sun's effect is important in all aborts that result in return flight times greater than 30 hours, and the effect of the earth's oblateness on the vehicle is significant for the near earth aborts where the vehicle's radial velocity remains positive after the abort.

APPENDIX B

PRIMARY NAVIGATION SYSTEM

The primary navigation system assumed in this study incorporates the optimal filter theory developed in reference 7. The system inputs consist of imperfect sextant angle observations between known stars and the earth and moon, and the principal output is the "best estimate" of the vehicle's current state. Part of the system is a subroutine that integrates the four-body equations of motion making it possible to compute the vehicle's state at any time by integrating the current state ahead. A block diagram of the system is shown in sketch (g). The system uses, as initial values for the equations of

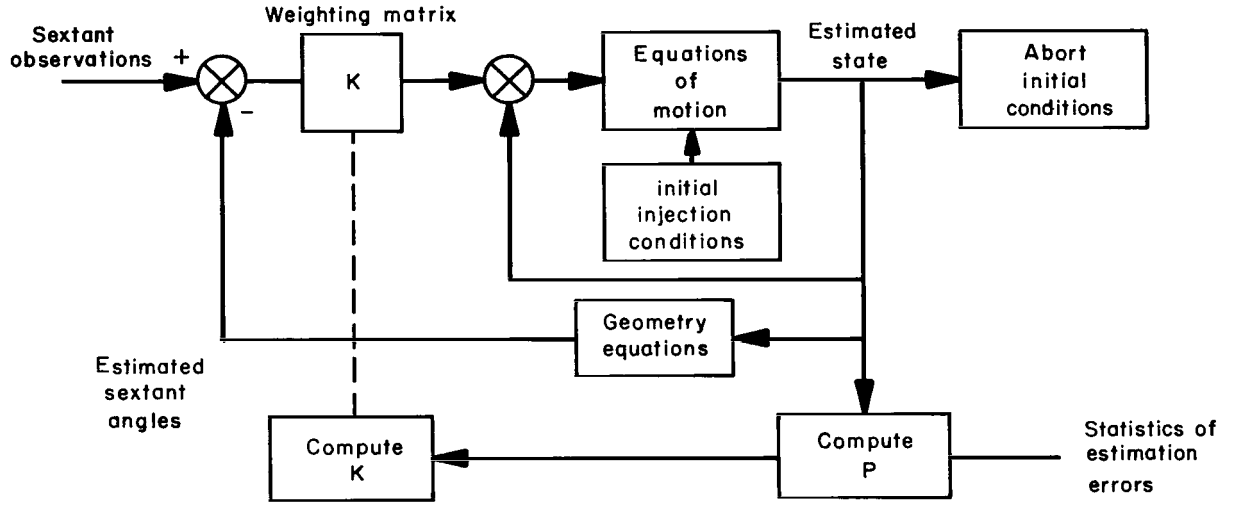

Sketch (g)

motion, the best estimate of the vehicle's state at injection. The reference injection conditions can be taken as the initial values if ground tracking or boost guidance is not available. These injection conditions are integrated ahead to the first two abort ranges, and the abort initial conditions are stored at each of these points. After storing the abort conditions, the integration is initiated again and updated to the observation time. The gain K is zero except when observations are made. At some time, t_k, when an observation is made, the observed angle is compared with the estimated angle computed from the estimated state at the observation time. The difference is weighted by the matrix $K(t_k)$ to produce an incremental change in the estimated state variables at time t_k. The new state then serves as new initial conditions on the equations of motion which are integrated to the following two abort ranges for determining improved abort initial conditions. Each time an observation is made this process is repeated, and as the first abort point is approached, it is dropped and the following one is picked up. Thus, the abort initial conditions are always available for two consecutive abort points.

The weighting matrix $K(t_k)$ is the basic part of the estimation procedure and is computed from equations given in reference 7. For solution these equations require, in addition to the equations of motion, the relations between the observables and the state variables (geometry equations), and the statistics of injection errors and instrumentation errors. Involved as an intermediate step in the calculation of $K(t_k)$ is the computation of the covariance matrix of estimation errors, $P(t)$, which is a description of the statistics of the errors in the estimate and is therefore quite useful as a measure of the performance of the system.

The trajectory determination system, of course, operates as an integral part of the complete vehicle guidance and control system and must take into account the intermittent application of impulsive velocity corrections during the normal mode of operation. When such corrective action is taken, the measured value of this action is introduced directly into the system as an instantaneous change in the estimate of the state, and the covariance matrix of the error in the measured value of the corrective action adds directly to P. Thereafter the system continues with its observation routine just as before with no loss of information due to the control action.

APPENDIX C

EQUATIONS OF MOTION

In the development of the equations of motion, a restricted four-body system was assumed with a spherical and homogeneous sun and moon. The second and fourth harmonic terms of the earth's oblateness are included. A geocentric Cartesian coordinate system is used with the Z axis along the earth's polar axis, positive to the north. The positive X axis is in the direction of the vernal equinox and the Y axis is oriented to form the right-hand system shown in sketch (h).

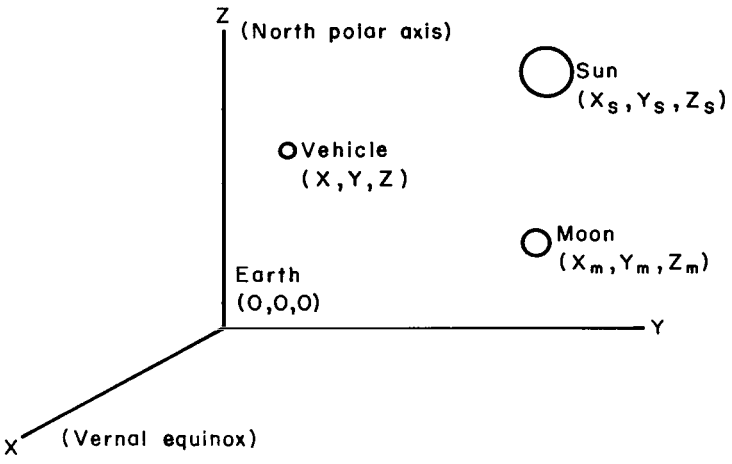

Sketch (h)

The equations of motion are derived by methods given in reference 8. They are as follows:

$$\ddot{X} = -\frac{\mu_e X}{R^3}\left\{\left[1 + J\left(\frac{a}{R}\right)^2\left(1 - 5\frac{Z^2}{R^2}\right)\right] + K\left(\frac{a}{R}\right)^4\left[\frac{1}{2} - 7\frac{Z^2}{R^2}\left(1 - 1.5\frac{Z^2}{R^2}\right)\right]\right\}$$

$$-\frac{\mu_m}{\Delta_m^3}(X - X_m) - \frac{\mu_m X_m}{R_m^3} - \frac{\mu_s(X - X_s)}{\Delta_s^3} - \frac{\mu_s X_s}{R_s^3}$$

$$\ddot{Y} = -\frac{\mu_e Y}{R^3}\left\{\left[1 + J\left(\frac{a}{R}\right)^2\left(1 - 5\frac{Z^2}{R^2}\right)\right] + K\left(\frac{a}{R}\right)^4\left[\frac{1}{2} - 7\frac{Z^2}{R^2}\left(1 - 1.5\frac{Z^2}{R^2}\right)\right]\right\}$$

$$-\frac{\mu_m}{\Delta_m^3}(Y - Y_m) - \frac{\mu_m Y_m}{R_m^3} - \frac{\mu_s(Y - Y_s)}{\Delta_s^3} - \frac{\mu_s Y_s}{R_s^3}$$

$$\ddot{Z} = -\frac{\mu_e Z}{R^3}\left\{\left[1 + J\left(\frac{a}{R}\right)^2\left(3 - 5\frac{Z^2}{R^2}\right)\right] - K\left(\frac{a}{R}\right)^4\left[1.5 - 7\frac{Z^2}{R^2}\left(10 - 9\frac{Z^2}{R^2}\right)\right]\right\}$$

$$-\frac{\mu_m}{\Delta_s^3}(Z - Z_m) - \frac{\mu_m Z_m}{R_m^3} - \frac{\mu_s(Z - Z_s)}{\Delta_s^3} - \frac{\mu_s Z_s}{R_s^3}$$

where

$$R = \sqrt{X^2 + Y^2 + Z^2}$$

$$R_m = \sqrt{X_m^2 + Y_m^2 + Z_m^2}$$

$$R_S = \sqrt{X_S^2 + Y_S^2 + Z_S^2}$$

$$\Delta_m = \sqrt{(X - X_m)^2 + (Y - Y_m)^2 + (Z - Z_m)^2}$$

$$\Delta_S = \sqrt{(X - X_S)^2 + (Y - Y_S)^2 + (Z - Z_S)^2}$$

$$\mu_e = 3.986031 \times 10^5 \text{ km}^3/\text{sec}^2$$

$$\mu_m = 4.8938269 \times 10^3 \text{ km}^3/\text{sec}^2$$

$$\mu_S = 1.3253 \times 10^{11} \text{ km}^3/\text{sec}^2$$

$$a = 6378.165 \text{ km}$$

$$J = 1.62346 \times 10^{-3}$$

$$K = 8.849 \times 10^{-6}$$

The equations of motion for the vehicle are solved by means of a Cowell "second-sum" method. A fourth-order Runge-Kutta method is used to start the integration and to change the step size during the flight. The positions of the sun and moon are obtained by interpolation of data from magnetic tape ephemerides. Within the sphere of influence of the moon, a lunar radius of 66,000 km, the origin of coordinates is translated to the center of the moon.

REFERENCES

1. Merrick, Robert B.; and Callas, George P.: Prediction of Velocity Requirements for Minimum Time Aborts From the Midcourse Region of a Lunar Mission. NASA TN D-1655, 1963.

2. Callas, George P.; and Merrick, Robert B.: A Manual Abort Technique for the Midcourse Region of a Lunar Mission. Paper presented at the AIAA Second Manned Space Flight Symposium, Dallas, Texas, April 22-24, 1963.

3. White, John S.; Callas, George P.; and Cicolani, Luigi S.: Application of Statistical Filter Theory to the Interplanetary Navigation and Guidance Problem. NASA TN D-2697, 1965.

4. Wong, Thomas J.; and Sly, Robert E.: The Effect of Lift on Entry Corridor Depth and Guidance Requirements for the Return Lunar Flight. NASA TR R-80, 1960.

5. Cicolani, Luigi S.: Linear Theory of Impulsive Velocity Corrections for Space Mission Guidance. NASA TN D-3365, 1966.

6. Wingrove, Rodney C.: Survey of Atmosphere Reentry Guidance and Control Methods. AIAA J., vol. 1, no. 9, Sept. 1963, pp. 2019-2029.

7. Smith, Gerald L.; Schmidt, Stanley F.; and McGee, Leonard A.: Application of Statistical Filter Theory to the Optimal Estimation of Position and Velocity on Board a Circumlunar Vehicle. NASA TR R-135, 1962.

8. Moulton, Forest Ray: An Introduction to Celestial Mechanics. Second ed., The Macmillan Co., 1959.

TABLE I.- OBSERVATION AND VELOCITY CORRECTION SCHEDULE FOR REFERENCE LUNAR TRAJECTORY

Time from injection, hr	Number of observations	Spacing of observations, hr	Total observations taken	Type of action	Observed bodies	
					Star	Body
0.5	4	0.5	4	Observation	Markab	Earth
2.5	4	.5	8	↓	Alpheratz	Earth
4.5	1	---	9	↓	Shaula	Moon
5.0	4	.5	13	↓	Alpheratz	Earth
7.0	1	---	14	↓	Shaula	Moon
7.5	2	1.0	16	↓	Alpheratz	Earth
9.0		---	---	Velocity correction	---	---
9.5	2	.5	18	Observation	Alpheratz	Earth
10.5	1	---	19	↓	Shaula	Moon
11.0	1	---	20	↓	Alpheratz	Earth
12.0	2	1.0	22	↓	Hamal	Earth
15.0	2	1.0	24	↓	Hamal	Earth
20.0	2	1.0	26	↓	Hamal	Earth
25.0	2	1.0	28	↓	Hamal	Earth
30.0	1	---	29	↓	Antares	Moon
34.0	1	---	30	↓	Hamal	Earth
37.0	4	2.0	34	↓	Hamal	Earth
45.0	1	---	35	↓	Antares	Moon
46.0	3	1.0	38	↓	Hamal	Earth
49.0	1	---	39	↓	Antares	Moon
50.0				Velocity correction	---	---
51.0	1	---	40	Observation	Antares	Moon
52.0	1	---	41	↓	Hamal	Earth
53.0	1	---	42	↓	Antares	Moon
55.0	1	---	43	↓	Hamal	Earth
57.0	2	1.0	45	↓	Antares	Moon
60.0	5	2.0	50	↓	Antares	Moon
69.0		---		Velocity correction	---	---

Star	Catalog number[a]
Markab	32149
Shaula	23769
Alpheratz	127
Hamal	2538
Antares	22157

[a]Atlas Coeli II Katalog 1950.0 by Antonin Becvar

TABLE II.- DESCRIPTION OF THE ABORT TRAJECTORIES

Abort point	Abort V, km/sec	Range from earth, km	Landing site[a]	Time, hr		
				Injection to abort	Abort to perigee	Injection to perigee
1	1.71	40,000	1	2.065	13.646	15.711
2	1.63	90,000	2	6.511	25.395	31.906
3	1.78	125,000	1	10.610	29.050	39.660
4	1.73	155,000	3	14.732	34.980	49.712
5	1.81	180,000	2	18.596	37.107	55.703
6	1.81	205,000	1	22.854	40.754	63.608
7	1.74	230,000	3	27.521	46.103	73.624
8	1.76	250,000	2	31.556	48.093	79.649
9	1.74	270,000	1	35.874	51.713	87.587
10	1.65	290,000	3	40.483	57.071	97.554
11	1.88	308,000	3	44.893	52.484	97.377
12	1.90	325,000	2	49.291	54.175	103.466
13	1.84	340,000	1	53.363	58.111	111.474
14	1.74	355,000	3	57.609	63.822	121.431

[a]Landing sites:

1. East of Cuttack, India
2. Near Honolulu, Hawaii
3. Near San Juan, Puerto Rico

TABLE III.- THE EMERGENCY CONDITIONS

Emergency point	Failure interval, hr	Abort point	Abort range, km
1	Inj. - 0.5	1	40,000
2	1.75 - 2.5	2	90,000
3	6.25 - 7.0	3	125,000
4	9.01 - 9.5	3	125,000
5	10.58 - 11.0	4	155,000
6	14.68 - 15.0	5	180,000
7	18.58 - 20.0	6	205,000
8	22.60 - 25.0	7	230,000
9	27.30 - 30.0	8	250,000
10	31.30 - 34.0	9	270,000
11	35.65 - 37.0	10	290,000
12	40.25 - 41.0	11	308,000
13	44.65 - 45.0	12	325,000
14	49.05 - 50.0	13	340,000
15	50.01 - 51.0	13	340,000
16	53.12 - 55.0	14	355,000

TABLE IV.- ROOT-MEAN-SQUARE MISS AT PERIGEE RESULTING FROM ERRORS CONSIDERED

Emergency condition	Abort point	RMS miss at time of reference perigee, km						RMS time deviation of actual perigee, sec
		Altitude miss due to errors in:			Total altitude miss	Total downrange miss	Total crossrange miss	
		Knowledge of state vector	Vernier thrusting	Delay in thrusting				
1	1	6.09	1.32	3.90	7.35	1347	1.37	127
2	2	7.19	2.68	1.65	7.84	2346	1.37	217
3	3	2.95	3.85	1.10	4.97	1161	.98	106
4	3	3.83	3.85	1.10	5.54	1434	1.10	132
5	4	3.57	4.62	.81	5.90	1293	.80	118
6	5	3.02	5.48	.73	6.30	1046	.52	96
7	6	3.04	6.20	.70	6.94	1062	.42	97
8	7	2.90	6.74	.67	7.37	1123	.40	102
9	8	2.80	7.37	.76	7.93	1051	.38	96
10	9	2.58	7.85	.80	8.30	579	.38	53
11	10	2.57	8.17	.81	8.60	663	.39	60
12	11	2.73	9.38	1.31	9.86	547	.64	50
13	12	2.74	9.95	1.59	10.44	558	.74	50
14	13	2.26	10.19	1.88	10.61	387	.73	35
15	13	2.36	10.19	1.88	10.63	385	.72	35
16	14	2.45	10.33	1.58	10.73	432	.63	39

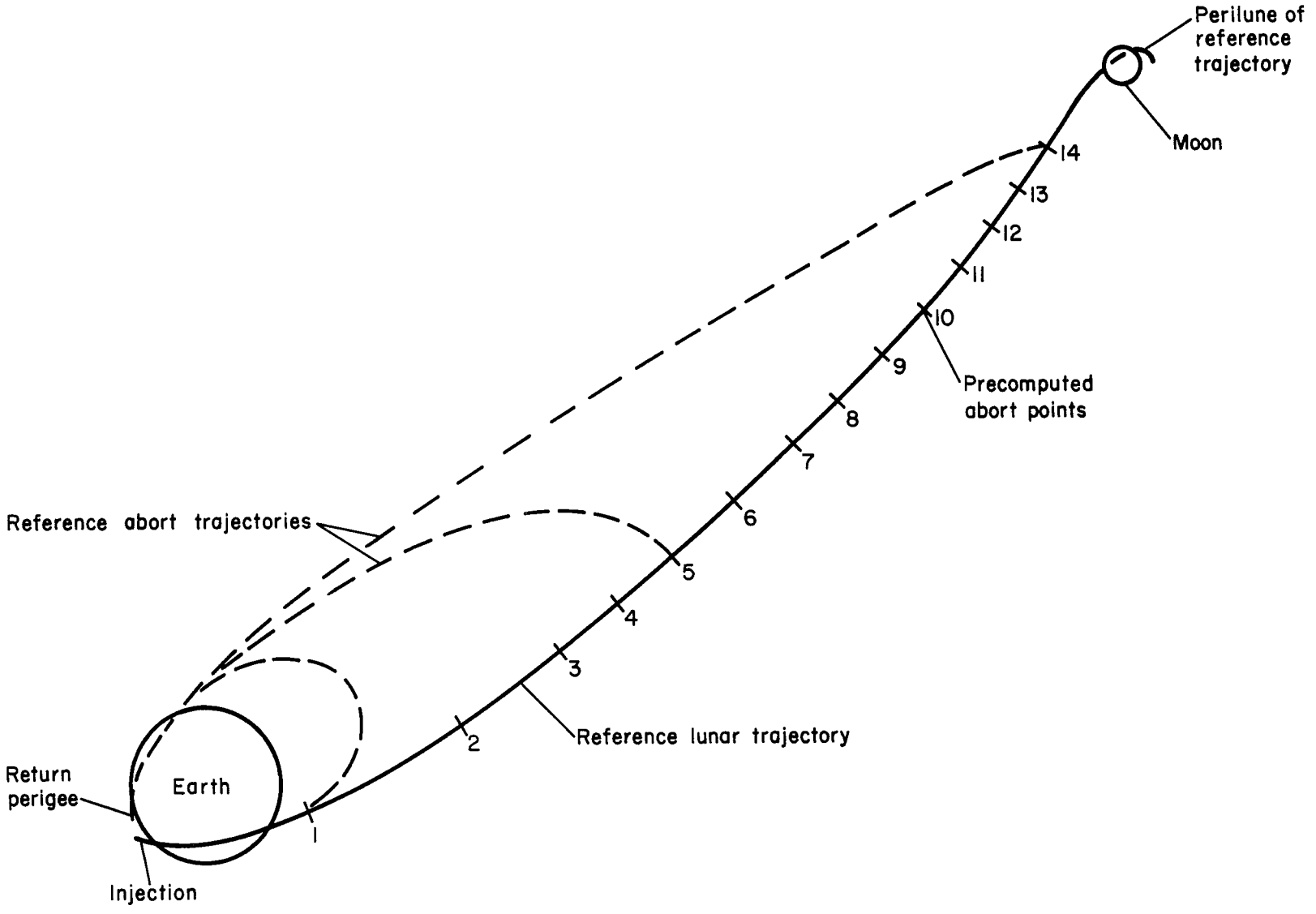

Figure 1.- Reference and abort trajectory profiles.

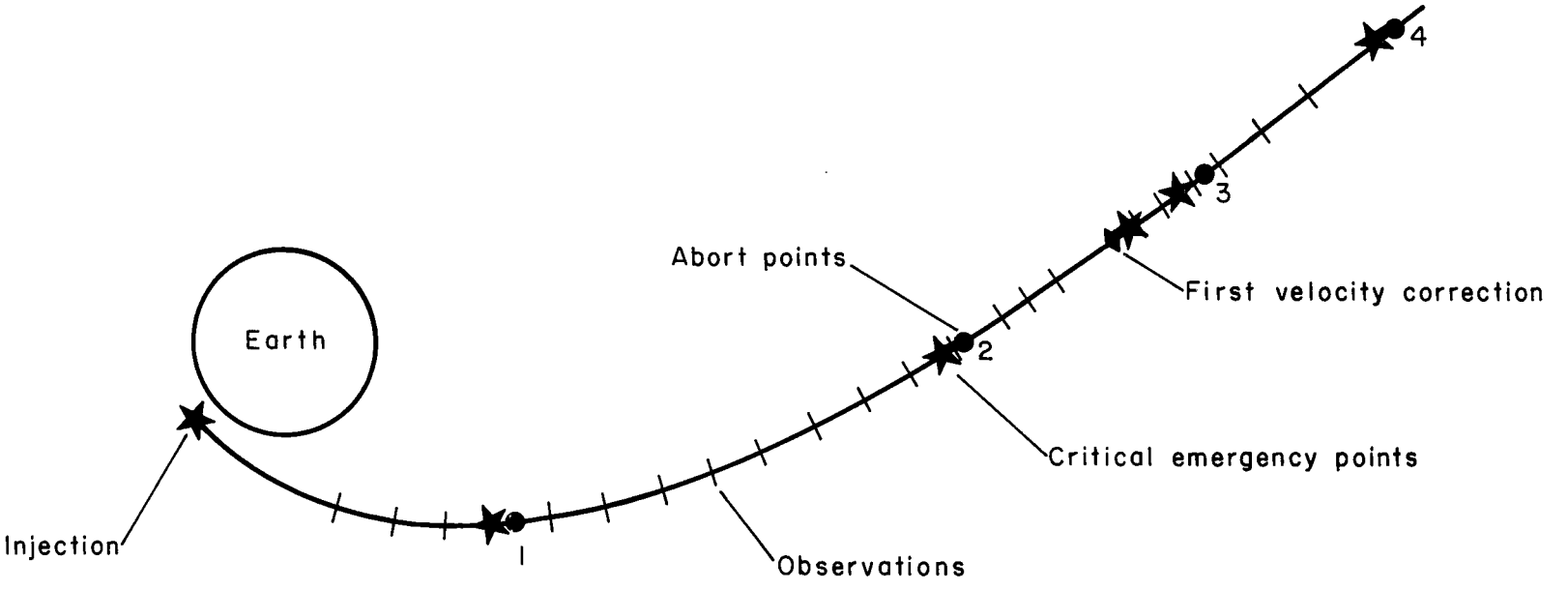

Figure 2.- Location of critical emergency points.

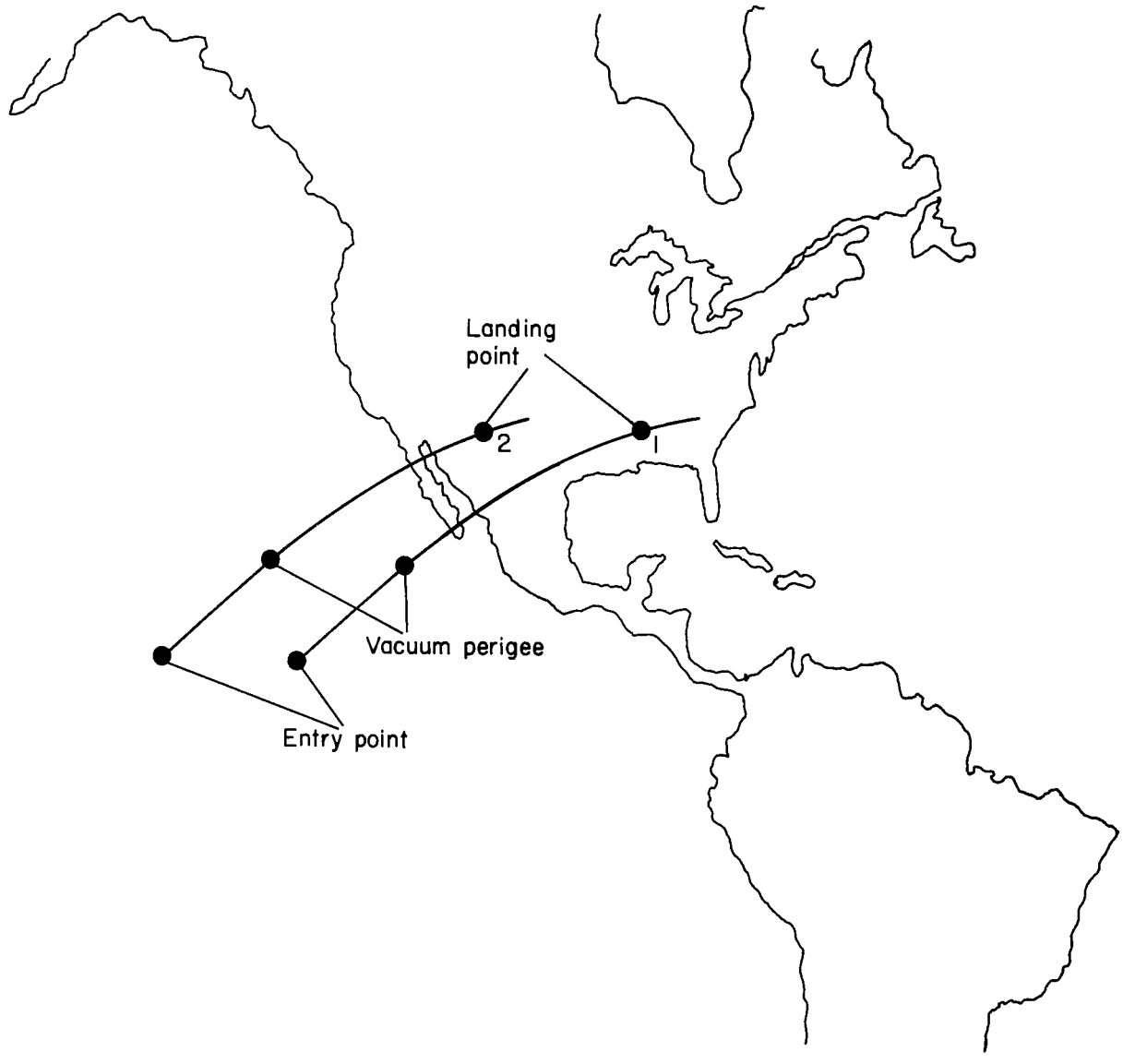

Figure 3.- Entry tracks of two trajectories whose entry time varies by 1 hr.

"The aeronautical and space activities of the United States shall be conducted so as to contribute . . . to the expansion of human knowledge of phenomena in the atmosphere and space. The Administration shall provide for the widest practicable and appropriate dissemination of information concerning its activities and the results thereof."

—NATIONAL AERONAUTICS AND SPACE ACT OF 1958

NASA SCIENTIFIC AND TECHNICAL PUBLICATIONS

TECHNICAL REPORTS: Scientific and technical information considered important, complete, and a lasting contribution to existing knowledge.

TECHNICAL NOTES: Information less broad in scope but nevertheless of importance as a contribution to existing knowledge.

TECHNICAL MEMORANDUMS: Information receiving limited distribution because of preliminary data, security classification, or other reasons.

CONTRACTOR REPORTS: Technical information generated in connection with a NASA contract or grant and released under NASA auspices.

TECHNICAL TRANSLATIONS: Information published in a foreign language considered to merit NASA distribution in English.

TECHNICAL REPRINTS: Information derived from NASA activities and initially published in the form of journal articles.

SPECIAL PUBLICATIONS: Information derived from or of value to NASA activities but not necessarily reporting the results of individual NASA-programmed scientific efforts. Publications include conference proceedings, monographs, data compilations, handbooks, sourcebooks, and special bibliographies.

Details on the availability of these publications may be obtained from:

SCIENTIFIC AND TECHNICAL INFORMATION DIVISION

NATIONAL AERONAUTICS AND SPACE ADMINISTRATION

Washington, D.C. 20546